ELSEVIER

PII: S0032-3861(96)00996-2

Polymer Vol. 38 No. 16, pp. 4139–4149, 1997

0032-3861/97/$17.00 + 0.00

Orientation and properties of sequentially drawn films of an isotactic polypropylene/ hydrogenated oligocyclopentadiene blend

Z. Bartczak*
Centre of Molecular and Macromolecular Studies, Polish Academy of Sciences, Sienkiewicza 112, 90-363 Łódź, Poland

and E. Martuscelli
Istituto di Ricerca e Tecnologia delle Materie Plastiche, CNR, Via Toiano 6, 80072 Arco Felice (NA), Italy
(Received 9 October 1996)

Films of isotactic polypropylene (iPP) and a blend of iPP and hydrogenated oligocyclopentadiene (HOCP) oriented by one-way (uniaxial) and two-way (sequential biaxial) drawing were studied. The mechanical and thermal properties of the oriented iPP and iPP/HOCP blends as well as orientation behaviour were investigated by means of mechanical tests, d.s.c. and small- and wide-angle X-ray scattering including the pole figures technique. It was found that drawing of iPP/HOCP blends to a high strain leads to the formation of highly oriented films having mechanical properties greatly improved compared to plain iPP oriented under the same conditions. The studies revealed in one-way drawn samples the multicomponent texture with chain axis, *c*, oriented in the machine direction, MD, for all texture components. The lamellae are oriented with normals parallel to the *c* direction. Due to differences in the amorphous phase content the texture in the blend samples is less developed than in deformed plain iPP. The subsequent drawing along the transverse direction, TD, leads to the reorientation of the *c* axis towards the TD, the sharpening of texture and the destruction of the lamellar structure. It was found that the major deformation mechanisms active in iPP and iPP/HOCP blends are: the crystallographic slips systems of (010)[001], (100)[001], (110)[001] and {110} twinning modes. In addition the interlamellar sliding is active as the main deformation mechanism in the amorphous phase. The (010)[001] system is the easiest of the slip systems active and dominates the other mechanisms. ©1997 Elsevier Science Ltd.

(Keywords: blends; polypopylene; plastic deformation; orientation)

INTRODUCTION

Easy processing, extensive applicability and the relative low cost of isotactic polypropylene (iPP) have resulted in a very high annual production and wide use of this polymer by itself as well as in various blends. In particular, the films of iPP blended with hydrogenated oligo(cyclopentadiene) (HOCP) were introduced several years ago into the packaging industry. These films have improved mechanical properties and a reduced permeability of oxygen and aroma as compared to films of just iPP[1,2]. HOCP is an amorphous resin miscible in any proportion with isotactic polypropylene with its glass transition temperature above that of iPP and can act as an antiplasticizer for the iPP homopolymer.

The iPP/HOCP blends and commercial isotropic films prepared from these blends have been studied intensively in the past[1–7]. It was found, that under some thermal conditions iPP and HOCP are completely miscible in the melt. However, a certain temperature and composition range was found within which a phase separation occurs. The existence of both the upper and lower cloud point curves was detected for that system[7]. The solid iPP/HOCP blend comprises of the crystalline fraction of plain iPP and the amorphous part which can be either in a single phase formed by iPP and HOCP molecules or in two phases of separated iPP and HOCP components depending on the cooling rate. The constitution of the amorphous phase depends on the thermal history of the sample. The crystallization of iPP from the homogeneous melt of iPP/HOCP blend is strongly affected by the presence of the HOCP component, especially at very high cooling rates. Under such conditions the iPP macromolecules do not crystallize in the usual monoclinic α form but solidify into a smectic modification[7]. This is due to substantially reduced mobility of iPP molecules in the blend as compared to a plain homopolymer at the same temperature—the glass transition temperature of the blend is reasonably higher than that of plain iPP[7].

The aim of this study was to investigate the plastic deformation of the iPP/HOCP blend and the properties of the resulting oriented films. The film samples designed for deformation study were prepared under thermal conditions such that phase separation within amorphous component did not occur. In this way the basic difference between plain iPP and the iPP/HOCP blend was in the amount and the properties of the amorphous phase.

* To whom correspondence should be addressed

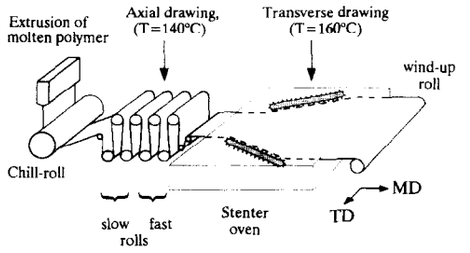

Figure 1 Experimental setup for extrusion of the film and its sequential two directional drawing

This, in turn, allowed the study of the influence of the amorphous phase on the deformation behaviour of the crystalline fraction of the material and the resulting properties of the films after deformation.

EXPERIMENTAL

Materials

The materials used were: commercial iPP, Moplen T305, Montedison, with M_w 3.0×10^5 g mol^{-1}, and the hydrogenated mixture of isomers of oligocyclopentadiene (HOCP), Escorez 5120 of Esso Chemicals Co., with M_w 630 g mol^{-1}, $T_g = 85°C$ and density $\rho = 1.07$ g cm^{-3}.

Blend preparation

The blend samples were prepared by extrusion of two components in a corotating twin-screw extruder at 240°C. After extrusion the extrudate was quickly cooled down to the room temperature and pelletized. The compositions of the prepared iPP/HOCP blend were: 100/0, 90/10, 80/20 and 70/30 (wt/wt).

Preparation of the oriented films

The initial isotropic films were prepared by extrusion of the blend in a single-screw extruder using a 25 cm wide slot-die at *ca* 245°C. The molten material was solidified in the form of a 1 mm thick film on a rotating chill-roll drum half-immersed in a water bath. The temperature of the roll was kept at 40°C. The obtained isotropic foil was subsequently stretched uniaxially in the direction of extrusion in a system of slow and fast rolls. The temperature within the deformation zone was maintained at 140°C. The velocity of the fastest roll was selected to obtain an extension ratio of 5/1. In the next step the film was stretched transversely by a stenter. This second, transverse stretching with extension ratio up to 8/1 was performed at 155–160°C. *Figure 1* shows the extrusion and orientation process. After each step of processing (solidification, axial stretching, transverse stretching) a sample of the blend was taken for further investigation. These samples will be referred to as unoriented, one-way (or uniaxially) drawn and two-way (or biaxially) drawn samples, respectively. The strain imposed on investigated samples during the orientation process will be described as 0×0 for unoriented (the first and second numbers refer to the strain in the machine direction, MD, and transverse direction, TD, respectively), 4×1 for one-way drawn and 4×7 for two-way drawn samples.

Measurements

A DuPont TA-2000 differential scanning calorimeter (d.s.c.) was used to study the melting behaviour of the specimens. The heating rate was 5°C min^{-1}. For calculation of the overall crystallinity of polypropylene from d.s.c. data the heat of fusion of 100% crystalline polypropylene was assumed at $\Delta H_f = 209$ J g^{-1} [8].

Mechanical tests of the oriented blend samples were carried out in the tensile mode at room temperature using a Model 1122 Instron tensile testing machine. Oar-shaped tensile specimens with a gauge length of 20 mm and a width of 4 mm (according to DIN 53504) were cut out from the unoriented and oriented films with the orientation parallel or perpendicular to the machine direction, MD (i.e. direction of the first drawing). The deformation rate was 10 mm min^{-1} in all tests.

The orientation of isotactic polypropylene crystalline component in the deformed blend samples was studied by means of X-ray diffraction measurements. A WAXS system consisting of a computer controlled pole figure device associated with a wide angle goniometer (DRON) coupled to an X-ray generator operating at 30 kV and 30 mA (CuK_α radiation, filtered electronically and by Ni filter) was used for X-ray measurements. The complete pole figures were obtained for the projection of Euler angles of crystal orientation with respect to the incident beam, α (polar angle) from 0° to 90° and β (azimuthal angle) from 0° to 360°, both in 5° intervals. The following diffraction reflections from the monoclinic crystal structure of polypropylene were analysed: (110), (040), (130), (060) and (113) (diffraction angle, $2\Theta \approx 14.1$, 16.9, 18.5, 25.5 and 42.5°, respectively). The construction of full pole figures required the connection of X-ray data collected in the reflection and transmission modes. The connecting angle α_c was 50°, i.e. the reflection mode was used for $\alpha = 0$–50° and the transmission mode for $\alpha = 50$–90°. The slit system of the diffractometer was always adjusted to measure the integral intensity of the appropriate diffraction peak. The necessary corrections for background scattering and sample absorption were introduced. The diffraction data were further corrected for the X-ray beam defocusing and other instrumental effects using the data obtained for identical experimental conditions for random (unoriented) standard specimen of iPP of the same thickness as the measured samples[9]. The pole figure plots were generated by the program POD, a part of the popLA package (Los Alamos National Laboratory, Los Alamos, New Mexico). All pole figures were plotted in a stereographic projection using linear intensity scale. Prior to plotting the calculated pole densities were self-normalized to the random pole distribution and then plotted in the units of multiplication of a density of random distribution (m.r.d.; 1 is equal to the density of random distribution).

Two-dimensional small-angle X-ray scattering (SAXS) patterns were recorded using a Siemens Hi-Star area detector controlled by a GADDS software coupled to a 18 kW rotating anode X-ray source (CuK_α radiation; Rigaku RV-300). The collimator system provided a point focus with a beam diameter of less than 1 mm. The distance between the sample holder and the detector was chosen to be 125 cm. The exposition times varied within the range from 30 min to 1 h.

RESULTS AND DISCUSSION

Figure 2a shows the dependence of the crystallinity degree of the iPP component in the blend on its composition for unoriented, one-way (uniaxially)

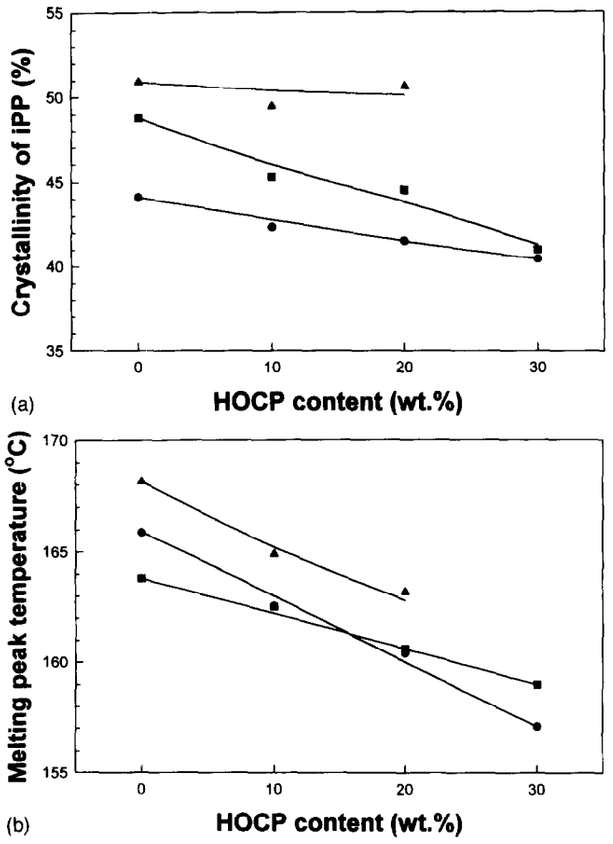

Figure 2 Dependence of the crystallinity degree of the iPP component in the iPP/HOCP blend (a) and the melting peak temperature (b) on the blend composition, determined from the d.s.c. data. (●) Unoriented samples; (■) one-way drawn samples; (▲) two-way drawn samples

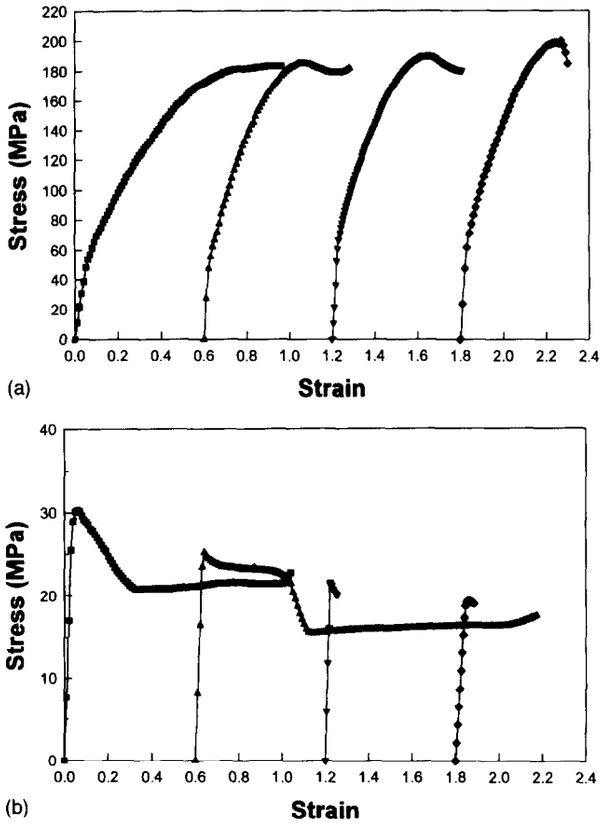

Figure 3 Typical stress–strain (engineering) curves for one-way drawn samples of iPP/HOCP blend obtained in tensile tests in the machine direction, MD (a) and in the transverse direction, TD (b). (■) 100/0, (▲) 90/10, (▼) 80/20, (◆) 70/30 iPP/HOCP blend. The subsequent curves were shifted along the strain axis for clarity

drawn and two-way (biaxially) drawn iPP/HOCP films, while *Figure 2b* presents the dependence of melting peak temperatures on the blend composition for the same samples, all obtained from the d.s.c. data. *Figure 2a* shows that in the unoriented samples the crystallinity of iPP component decreases with increasing HOCP content in the blend. This indicates the restraining effect of molecularly dispersed HOCP on the crystallization of iPP component. The same trend is reflected in crystallinity degree in both sets of oriented samples. However, the crystallinity of the iPP component increases markedly with increasing deformation. Similar effect can be observed in the melting behaviour (cf. *Figure 2b*). These effects are primarily the result of an annealing accompanying the deformation process: the temperature was set to 140°C at the first drawing step and to 160°C at the second, while the temperature of the chill-roll on which the unoriented foils had been solidified was kept at only 40°C. On the other hand, in the uniaxially oriented samples the crystallinity degree and the melting temperature decrease somewhat faster with increasing HOCP content than in the unoriented blend samples, whereas in the biaxially oriented samples the crystallinity degree of iPP component remains nearly constant with composition (of course, the overall crystallinity of the blend decreases with increasing HOCP content). The melting temperature of biaxially oriented samples decreases with increasing concentration of HOCP at a similar rate to that observed in unoriented samples. Such behaviour can be attributed, in addition to the annealing effect, to the differences in the deformation conditions (different initial morphology and different strain imposed) of the blends of various compositions during the two deformation steps.

Figure 3 shows typical stress–strain curves obtained in tensile experiments for one-way (uniaxially) oriented blend samples. The direction of tension was parallel to the machine direction, MD (which is the direction of first draw; see *Figure 3a*), or to the transverse direction, TD (*Figure 3b*). It was observed that samples tested along the MD elongated without the formation of a neck up to the fracture, while in those tested along the TD a neck was formed during elongation. Necking is accompanied by a substantial reorientation which allows further drawing. In the 9/1 iPP/HOCP blend sample elongated along the TD, a double necking was observed.

Similar tensile tests along the MD and TD were performed for two-way (biaxially) oriented blend films. Typical stress–strain curves for these samples are presented in *Figures 4a* and *b*, respectively. The biaxially oriented samples elongated with formation of a neck when tested along the MD (direction of the first-stage draw) and without necking when tested along the TD (direction of the final draw), cf. *Figures 4a* and *b*.

From the measured stress–strain curves the Young's modulus, E, yield stress, σ_y, ultimate strength, σ_m and elongation at break, ϵ_b, were determined. The yield stress was calculated as the stress corresponding to maximum

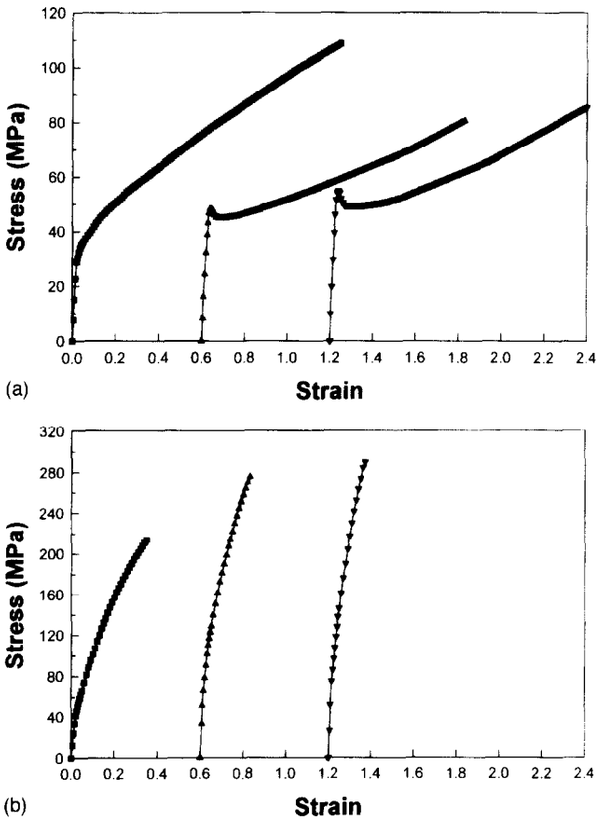

Figure 4 Typical stress–strain (engineering) curves for two-way drawn samples of iPP/HOCP blend obtained in tensile tests in the machine direction, MD (a) and in the transverse direction, TD (b). (■) 100/0, (▲) 90/10, (▼) 80/20, iPP/HOCP blend. The subsequent curves were shifted along the strain axis for clarity

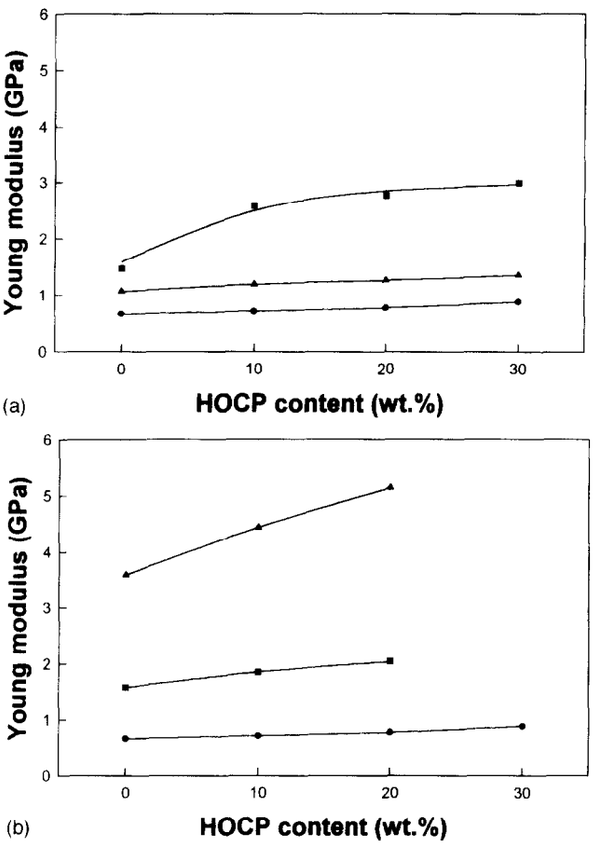

Figure 5 The dependence of Young modulus on the blend composition determined for one-way drawn (a) and two-way drawn blend films (b). Moduli of unoriented samples are shown for reference. (●) Unoriented samples; (■) test in machine direction; (▲) test in transverse direction

on load–extension curves for those specimens which showed necking and accompanying load drop, whereas for those not exhibiting necking the yield stress was taken as the stress where the two tangents to the initial and subsequent parts of the load–extension curve intersect[10]. *Figures 5–8* present the determined values of E, σ_y, σ_m and ϵ_b as the function of blend composition. The same parameters determined for unoriented blends are also shown in these figures for reference. The figures demonstrate that for all compositions studied the oriented films have markedly improved mechanical properties in both MD and TD directions compared to unoriented samples of the same composition, except for the elongation at break (cf. *Figure 8*), which is much lower than in unoriented materials[1] (note the additional drop in the ϵ_b down to less than 10% for one-way drawn samples containing 20–30 wt% of HOCP when tested along the TD). Moreover, the Young modulus, yield stress and ultimate strength in one-way drawn as well as two-way drawn samples increase strongly with increasing HOCP content in the blend, especially in the direction of sample orientation (i.e. MD for one-way drawn samples and TD for two-way drawn samples, respectively). The above results demonstrate that the addition of HOCP to iPP greatly improves the performance of this polymer in the oriented state. Simultaneously, the processability of iPP/HOCP blends in the form of film is not degraded as well as the drawability as compared to plain iPP. The optimum amount of HOCP to obtain the oriented material with considerably improved mechanical properties seems to be around 20 wt%. One should note, however, that the transverse drawing of the one-way oriented blend containing 20 wt% or more of HOCP is difficult at room or moderately high temperature—the material breaks prematurely, before any serious reorientation can occur (cf. *Figure 8a*). It was found that in order to reach high strain, transverse drawing must be carried out at a very high temperature, slightly below the melting point of iPP crystals.

The mechanical properties of two-way drawn samples in the direction of the final draw (TD) are much better than those drawn uniaxially, while in the MD they remain nearly the same as in uniaxially oriented samples. This is primarily due to the higher orientation of the material produced by the two-stage drawing process—the strain for two-way drawn samples was 4 × 7 with no contraction along the MD at the final drawing vs 4 × 1 for those drawn uniaxially.

The orientation behaviour of the blends studied and the influence of HOCP content on the deformation will be discussed below. The orientation of the iPP crystallites in the oriented blends was studied by means of a pole figure technique, while the lamellar orientation was investigated by small angle X-ray scattering (SAXS).

Figure 9 presents the pole figures of the (110), (040), (130), (060) and (113) crystallographic planes of monoclinic iPP crystals (α form), obtained for one-way

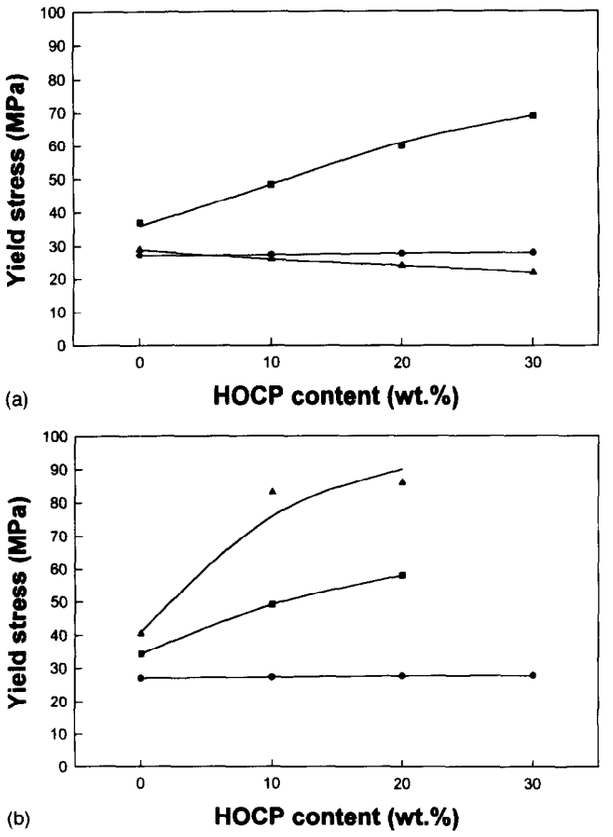

Figure 6 The dependence of yield stress on the blend composition determined for one-way drawn (a) and two-way drawn blend films (b). The yield stresses of unoriented samples are shown for reference. (●) Unoriented samples; (■) test in machine direction; (▲) test in transverse direction

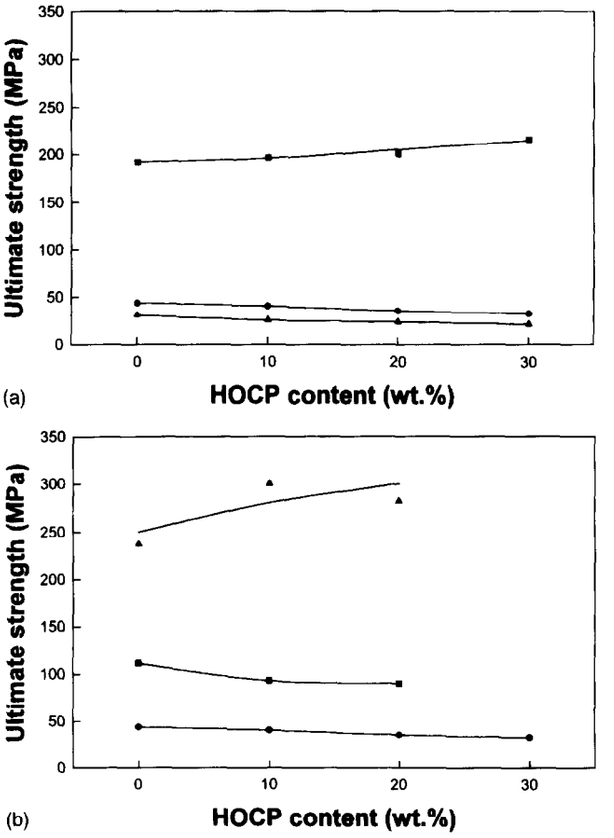

Figure 7 The dependence of ultimate strength on the blend composition determined for one-way drawn (a) and two-way drawn blend films (b). Ultimate strengths of unoriented samples are shown for reference. (●) Unoriented samples; (■) test in machine direction; (▲) test in transverse direction

(uniaxially) drawn plain iPP film. *Figure 10* presents a similar set of pole figures determined for one-way drawn 8/2 iPP/HOCP blend.

The diffraction peaks from the (110), (040) and (130) planes frequently overlap with their tails. Moreover, they are superimposed over an amorphous halo and reflections of (021) and ($\bar{1}$11) crystal planes (Bragg angles 16.2° and 18.2°, respectively). The overlapping of the (040) and (130) peaks is usually much stronger than the (110) and (040) peaks [distance between (040) and (130) peaks is merely 1.6°]. The diffraction intensities were determined during pole figure measurements using a wide receiving slit in order to obtain values of integral intensities (receiving slit used had an angular width of 1.3°). As no separation of the contribution of the neighbouring overlapping peak was possible for these data, both the (040) and (130) pole figures include some unknown contribution from the other planes, which make these figures less accurate than those measured for non-overlapped peaks. The pole figures obtained for the (110) plane, giving a very strong reflection, are much less influenced by the contribution of (021) and (040) planes and by the scattering from the amorphous phase than the (040) or (130) pole figures, but still, there is some level of uncertainty. For the reason of the limited accuracy of the (040) pole figure (which is the most influenced by the other peaks) we additionally measured the pole figure of (060) plane, which in the absence of errors should be identical to the (040) pole figure. The peak of the (060) plane is separated from its neighbours, but unfortunately it has much lower intensity than the (040) peak, thus the accuracy of the pole figure constructed for this plane is also limited. However, the analysis of all mentioned above pole figures together should lead to quite reasonable conclusions.

The pole figures referred to as ($\bar{1}$13) were constructed from the integral intensities of the diffraction peak placed near $2\Theta \approx 42.5°$. This peak results primarily from the diffraction on ($\bar{1}$13) planes ($2\Theta = 42.52°$), although its shape in oriented samples may suggest some contribution from other reflections. At the same location ($2\Theta = 42.50°$) one could expect the (031) reflection, which possibly occurs for the ordered stable α_2 modification of monoclinic iPP (symmetry group $P2_1/c$[11]. Since in the annealed samples this ordered form can be present in large quantity, the contribution produced by the (013) plane to the ($\bar{1}$13) peak can be significant. Another reflection in this range of 2Θ (at *ca* 41.9°) was reported for highly oriented iPP[12]. This reflection cannot be indexed as any reflection of the common crystallographic form of iPP. Its position is characteristic of a diffraction spacing equal to the monomeric repeat distance of polypropylene in the 3_1 helical conformation (2.17 Å). It was suggested that this peak can arise either from highly oriented molecules in the noncrystalline state[12] or, more probably, from a disordered crystal

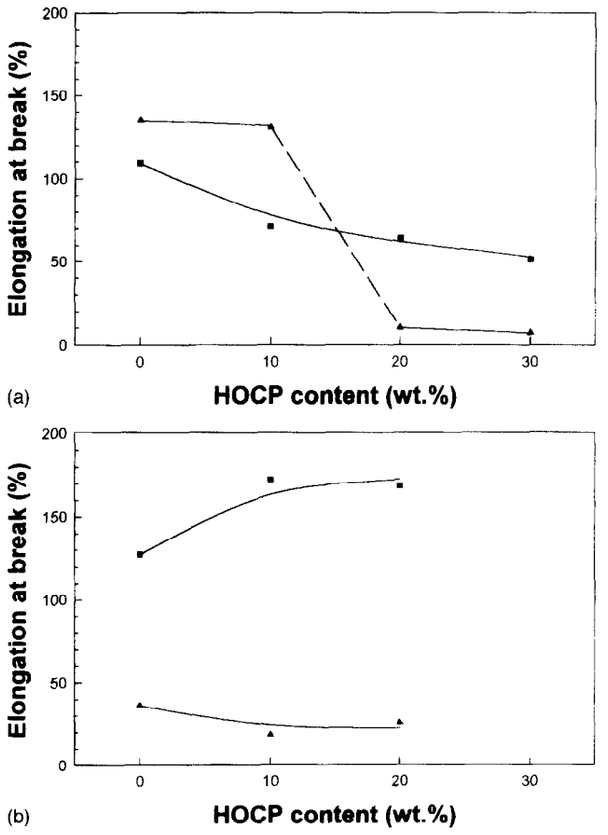

Figure 8 The dependence of elongation at break on the blend composition determined for one-way drawn (a) and two-way drawn blend films (b). (■) Test in machine direction; (▲) test in transverse direction

structure with reduced symmetry[12,13]. In the latter case there is also a possibility of the presence of a (003) peak of such a disordered structure at the position near $2\Theta = 42.3°$. In our data, we did not find any evidence of the mentioned reflection at 41.9°, but some distortion of the shape of the ($\bar{1}13$) peak observed in one-way drawn samples as well as the pole distribution in the respective pole figures may suggest the presence of the reflection of the (003) type. Despite the complexity of the peak referred to here as ($\bar{1}13$), it is the best possible experimental measure of the orientation of molecular axis in the crystalline phase of a sample containing iPP. The pole of the ($\bar{1}13$) plane is located only 5.8° away from the direction of the molecular axis, equivalent to the crystallographic c axis (and distanced 99.4° to the a^* axis and 84.2° to the b axis), while that of the (013) plane is also oriented 5.8° away from the c direction and forms an angle of 80.7° with the a^* axis and 84.2° with the b axis. The position of the hypothetical (003) pole of disordered structure should be located 9.3° away from c in the a^*–c plane (see *Figure 11* for the position of the discussed poles).

From *Figure 9* it is seen that for one-way drawn iPP samples normals to the ($hk0$) planes are clustered in the TD–ND plane, perpendicular to the MD (ND denotes normal direction, i.e. direction of the film thickness). In this plane the poles form a rather broad concentration maximum. The poles of the (040) plane form a broad maximum of distribution density resembling a fan centred in the ND. This fan extends up to ±45° from

Table 1 The expected positions of poles of the crystallographic planes studied for the postulated texture elements of one-way drawn samples

	(010)[001]	(100)[001]	(110)[001]	{110}
hkl	Angle between plane normal and ND-TD plane (°)			
110	72.6	17.4	0, 34.8	37.8, 72.6
(040), (060)	0	90	72.6	34.8
130	46.8	43.2	25.8, 29.4	12, 81.6
($\bar{1}13$)/(013)	9.4	80.6	63.2, 82	25.4, 44.2

ND towards TD. Two sets of smaller maxima in the (040) pole figure can be observed at *ca* 70° from ND towards TD and close to TD. In the (060) pole figure similar features can be found. In the pole figure constructed for the (110) plane the poles concentrate in a fan around the ND in the ND–TD plane. Within this region of concentration two distribution maxima of *ca* 40° from the ND can be distinguished. Two other maxima extend in the range 60°–90° from the ND. In the (130) pole figure the following maxima of the poles concentration can be found in a ND–TD plane: a broad one at *ca* 0°–45° range with two visible culminations near 10° and 45° from the ND and additionally a distinct maximum approximately 80° from the ND.

The analysis of the positions of maxima of pole distributions of the above discussed ($hk0$) planes leads to the conclusion that the texture of one-way drawn iPP sample consists of four components. All these components have a common direction of the c axis coinciding with the MD. These components are: (1) normals to the ($0k0$) planes (i.e. the b axis) oriented in the ND, with the a^* axis in the TD and the c axis in the MD, i.e. the (010)[001] texture; (2) normals to the ($0k0$) planes (i.e. the b axis) oriented in the TD, with the a^* axis in the ND and the c axis in the MD, i.e. the (100)[001] texture; (3) normals to the (110) or ($1\bar{1}0$) planes oriented along the ND and the c axis in the MD, i.e. the (100)[001] texture; (4) the {110} and {$1\bar{1}0$} twins of the crystals approaching the orientation of type (1), which can be denoted as the {110} texture. In all of these components two mirror orientations of the monoclinic unit cell with respect to the ND–MD plane are possible, thus there are as many as 12 basic orientations of the unit cell in the postulated texture of one-way drawn iPP. *Table 1* summarizes the positions of the poles of the planes of interest characteristic for the postulated three texture elements, expected on the basis of the geometry of the unit cell of α modification of polypropylene. The positions of the maxima in pole distributions observed experimentally agree very well with those reported in *Table 1* which proves the postulated texture. The pole figure measured for the ($\bar{1}13$)/(013) plane agrees with the postulated texture, except that there are additional distinct maxima located in the MD–TD plane *ca* ±10° from the MD towards the TD. These are neither the poles of ($\bar{1}13$) nor (013) planes of any of postulated texture elements because those poles should be 5.8° apart from the MD, which here is equivalent to the c axis. The possible explanation is that they originate from (003) reflection of the distorted crystals with the reduced symmetry—the pole of such planes in the texture of the (010)[001] type should be observed ±9.3° away from MD towards TD, which agrees well with the experimental ±10° deviation in the ($\bar{1}13$)/(013) pole figure.

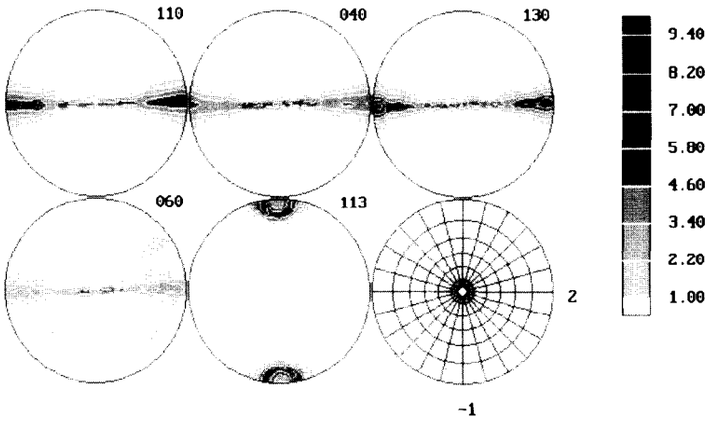

Figure 9 The pole figures of (110), (040), (130), (060) and ($\bar{1}$13) planes of monoclinic α form iPP for one-way drawn plain iPP, plotted in stereographic projection. The lower right plot show the 15° net of polar and azimuthal angles. The direction denoted as 1 on the plot is equivalent to the machine direction, MD, 2 is equivalent to the transverse direction, TD

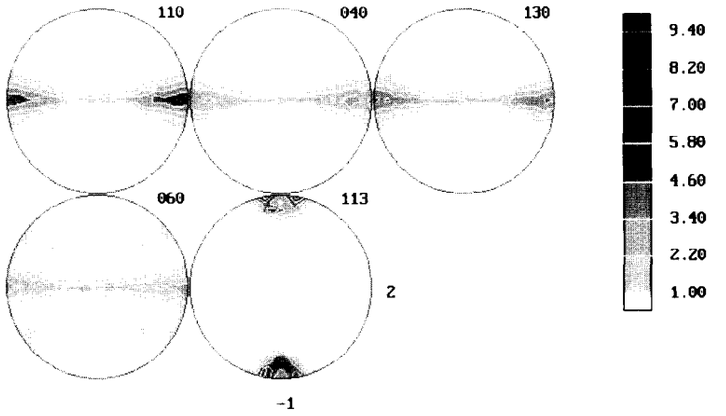

Figure 10 The pole figures of (110), (040), (130), (060) and ($\bar{1}$13) planes of monoclinic α form iPP for one-way drawn 8/2 iPP/HOCP blend, plotted in stereographic projection. The direction denoted as 1 on the plot is equivalent to the MD, 2 is equivalent to the TD

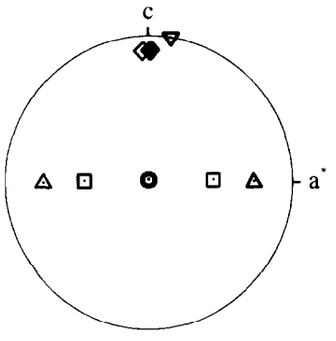

Figure 11 Calculated positions of poles of chosen crystallographic planes of an ideal monoclinic polypropylene shown in stereographic projection: ○ (040) plane; □ (130) plane; △ (110) plane; ◇ ($\bar{1}$13) plane; ◆ (013) plane of α_2 structure; ▽ (003) plane of hypothetical disordered crystal with reduced symmetry

The principal mechanisms responsible for the formation of the reported texture are most probably the crystallographic slips along the chain axis of the (010)[001] (100)[001] and (110)[001] systems as well as the {110} twinning occurring at latter stages of the drawing process in crystals with the (0k0) planes already oriented along the ND. According to the theoretical predictions the (010)[001] slip system should be the easiest one in polypropylene crystals, while the (100)[001] and (110)[001] systems should have higher critical resolved shear stresses[14]. The mentioned mechanisms are supplemented most probably by other slip systems (e.g. the (010)[001] transverse slip) as well as the mechanisms active in the amorphous phase (mainly interlamellar sliding).

The postulated deformation by the {110} twinning of the crystals oriented with their b axis near the ND needs a reasonable compressive stress acting along the direction close to the transverse direction or a tensile stress along the ND, similar to the {110} and {130} twinning modes operating in polyethylene[15]. During drawing, however, such stresses are unlikely to occur, because the stretched film was relatively wide (250 vs 1 mm of the initial thickness) and passed by several rolls in the drawing apparatus. The friction between the film and rolls as well as a small distance between those rolls prevented the film from contraction in the TD. Thus, the stress generated along the TD during drawing is rather tensile, which does not favour the discussed twinning. The situation changes beyond the last extension roll—the lateral constraints are no longer active in the oriented film and in the amorphous phase some restoring stresses are generated, which tend to cause the film to contract in the TD and

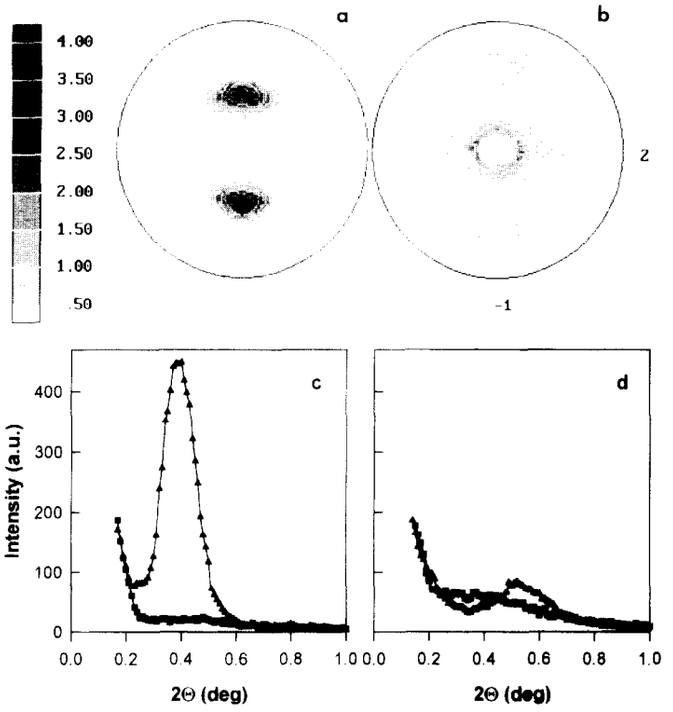

Figure 12 Two-dimensional SAXS patterns of one-way drawn plain iPP (a) and 8/2 iPP/HOCP blend (b). The cross-sections of these patterns along the MD (▲) and TD (■) are shown in (c) and (d), respectively

expand in the ND directions. Such stresses are equivalent to the compressive stress in the TD and to the tension in the ND. Their effect on the crystallites oriented with (0k0) planes in the film plane should be to induce the {110} twinning. Similar post-deformation behaviour was reported for polyethylene[15].

Figure 10 presents the set of pole figures of the (110), (040), (130), (060) and ($\bar{1}$13) planes measured for the sample of 8/2 iPP/HOCP blend oriented in one-step uniaxial drawing. These figures show similar features to those obtained for iPP, thus the blend sample has a texture consisting of the same elements as those present in plain iPP deformed under the same conditions. The difference between textures of these two samples is mostly in the heights of the respective maxima—the texture of the 8/2 blend is generally less developed than that of iPP—the maxima of pole orientation distributions in the blend are 20–30% lower than the respective maxima of the iPP sample (since all pole figures were self-normalized to the random crystal distribution it is possible to compare directly the two textures). Moreover, relations between the values of pole density at appropriate maxima of pole figures of the 8/2 blend suggest that the texture of this blend contains a lower fraction of the (100)[001] and (110)[001] elements than the texture observed in plain iPP. The above differences can be attributed to the presence of larger fraction of the amorphous phase in the blend sample and to the difference in properties of the amorphous phase (e.g. the difference in the stress necessary to activate plastic flow). Both samples were elongated to a strain equal to 4. At such moderate elongation the strain accommodated by the amorphous phase at the initial stages of the deformation process as well as during subsequent deformation of crystalline phase is relatively high. However, it seems that the deformation of amorphous phase is not saturated yet since a much higher strain could be achieved in iPP. Since the amount of the amorphous component in the blend is higher than in the case of plain iPP, it can accommodate a higher strain, hence the crystallites orient themselves less perfectly in the course of plastic deformation. Due to more extensive deformation of the amorphous phase the (100)[001] and (110)[001] slips, more difficult to activate than the easiest (010)[001] slip, are relatively less advanced in the blend at the strain reached and, consequently, these texture components in the blend are relatively weaker compared to the (010)[001] texture component, which apparently dominates the texture of the blend sample.

Figure 12 presents two-dimensional SAXS patterns of samples of one-way drawn iPP (*Figure 12a*) and the 8/2 blend (*Figure 12b*) as well as the cross-section scans of these patterns made along the MD and TD, respectively (*Figures 12c* and *d*). These figures show that in both samples the orientation of crystallites is accompanied by the orientation of the lamellar structure during the unidirectional deformation (a strain of 4 reached). The patterns are of the two-point type, which demonstrates that the lamellar structure was not destroyed in this step of orientation process but was transformed from the initial random orientation to an orientation with lamella normals, n, along the MD. Moreover, neither scattering pattern exhibits any scattering characteristic for the presence of voids, which additionally proves that the lamellae underwent rotation only, and not the major destruction which usually is accompanied by the formation of micro-voids. The maxima in the SAXS pattern of plain iPP observed in the MD are sharp and well developed, while in the other directions there is no scattering indicating lamellar structure (see *Figure 12c* showing the single scans of the 2-dimensional pattern along the MD and TD), which demonstrates that

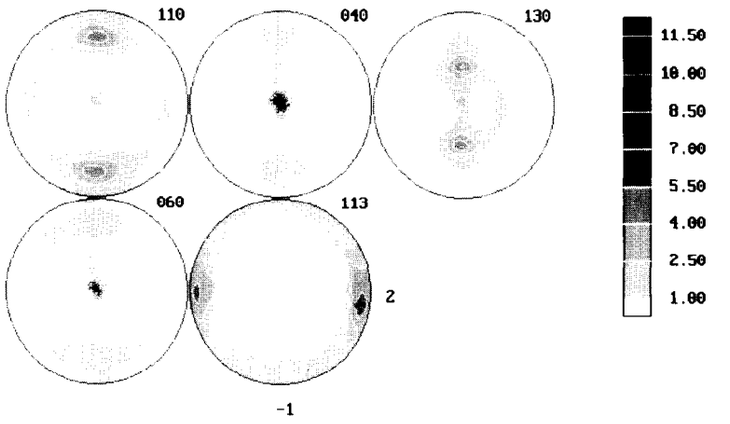

Figure 13 The pole figures of (110), (040), (130), (060) and ($\bar{1}$13) planes of monoclinic α form iPP for two-way drawn plain iPP, plotted in stereographic projection. The direction denoted as 1 on the plot is equivalent to the MD, 2 is equivalent to the TD

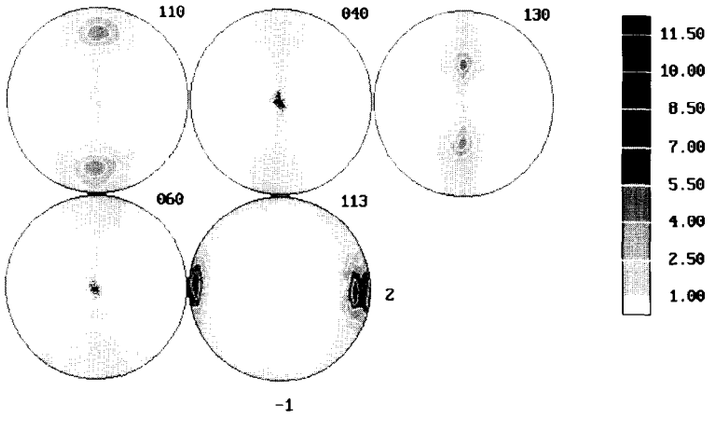

Figure 14 The pole figures of (110), (040), (130), (060) and ($\bar{1}$13) planes of monoclinic α form iPP for two-way drawn 8/2 iPP/HOCP blend, plotted in stereographic projection. The direction denoted as 1 on the plot is equivalent to the MD, 2 is equivalent to the TD

practically all lamellae became oriented perpendicularly to the MD (*n* parallel to the MD). In the unidirectional oriented sample of the 8/2 blend the main maximum also indicates the same lamellar orientation, but there is another, albeit weaker, lamellar scattering in the TD direction (see *Figures 12b* and *d*). That scattering can be the result of interlamellar sliding operating in the amorphous phase and causing the lamellae rotation to a final orientation with *n* parallel to the TD. As previously discussed, the fraction of the amorphous phase in the 8/2 blend is larger than in plain iPP and, moreover, its deformation here is relatively more advanced.

The intensities at the maxima of SAXS scattering of the blend sample are much lower than those of plain iPP. One reason for this effect is the lower diffraction contrast in the blend sample due to the higher density of the amorphous component loaded with HOCP which results in a lower difference of crystal and amorphous densities in the blend compared to iPP. The other reason may be the bimodal and less developed lamellar orientation as compared to that observed in plain iPP.

Another feature of the SAXS pattern of the blend is that the long period measured along the MD is much lower than the respective long period observed in plain iPP (16 and 24.5 nm, respectively) while that measured along the TD is comparable to plain iPP (*ca* 24 nm). The long period in the 8/2 blend is also lower than in iPP in raw undeformed films solidified at 40°C; LP = 10 and 12.5 nm for the blend and iPP, respectively[16]. During the draw at 140° the lamellae in both samples became considerably thicker due to annealing, but the origin of the large difference of the new long period values when observed along the MD and TD in the blend sample is still unclear.

Figures 13 and *14* present the sets of (110), (040), (130), (060) and ($\bar{1}$13) pole figures determined for two-way drawn iPP and 8/2 iPP/HOCP blend, respectively. Textures of both samples exhibit similar features and differ only in a few details. Due to the second drawing in the transverse direction crystallites reorient with their chain axis towards the TD. There is only a faint trace of the previous orientation in the MD as well as the reorientation path seen in plain iPP sample, absent in the blend. The texture of two-way drawn films is much better developed and sharper than that observed in one-way drawn samples. The intensity of the main maximum in the (040) pole figure is four times higher than in uniaxially drawn samples (26 m.r.d. comparing to 8.5 m.r.d. for two-way and one-way drawn iPP, respectively. *Figures 13* and *14* are plotted in a more detailed scale in order to visualize other texture details). Moreover, the positions and the heights of the distribution maxima indicate that the texture of the two-way

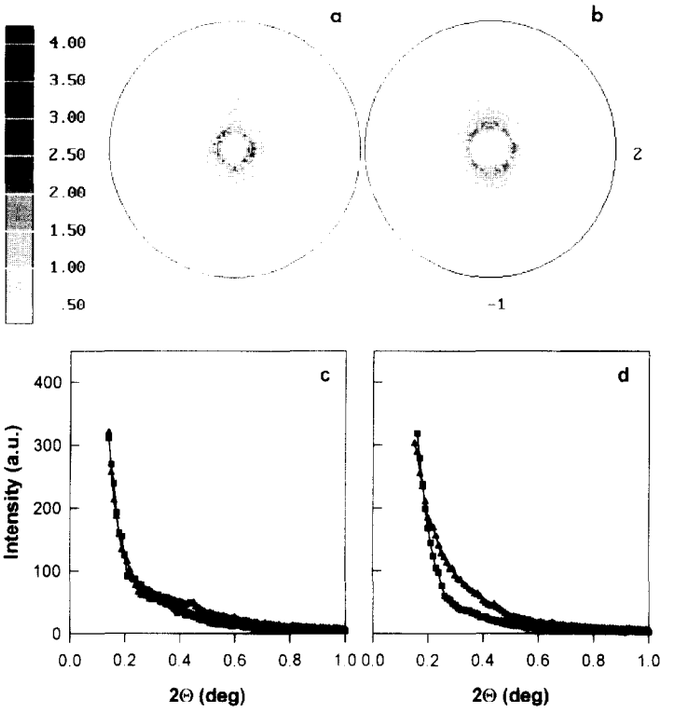

Figure 15 Two-dimensional SAXS patterns of two-way drawn plain iPP (a) and 8/2 iPP/HOCP blend (b). The cross-sections of these patterns along the MD (▲) and TD (■) are shown in (c) and (d), respectively

drawn samples constitutes only two components: very strong (010)[001] and much weaker (110)[001] textures. There is no evidence of (100)[001] and {110} twinning components. This suggests that the structure reorientation during the second drawing was realized almost entirely by the easiest (010)[001] slip system. The twinning component disappears from the texture probably due to annealing accompanying the second drawing. Under such conditions the crystal internal stresses could relax near the entrance to the stenter oven and the crystallites could then twin back to the (010) orientation. It is not clear, however, why during the second draw only the slips of (010)[001] and (110)[001] were active while there is no evidence of (100)[001] slip system activity. According to theoretical consideration (100)[001] has a lower critical resolved shear strain than (110)[001][14], thus it should win the competition and eventually eliminate (110)[001] at high strain, which disagrees with the observed final texture.

The pole figures constructed for ($\bar{1}13$) of two-way drawn samples do not show any peculiarities and agree completely with figures for (*hk*0) planes. The maximum interpreted for one-way drawn samples as being a result of diffraction on the (003) plane of disordered crystal structure disappears during the second drawing and only that originating from the diffraction on the (113) plane can be observed. This improvement of the crystal structure can be attributed to the annealing at high temperature (up to 155–160°C) prior to and during the second drawing, inducing transformation of these crystals back to the higher symmetry state.

The textures of two-way drawn iPP and 8/2 blend are almost identical. They both consist of the same two sharp texture components in similar proportions. The main (100)[001] orientation is developed to nearly the same level in both iPP and blend samples, which is contrary to the one-way deformed samples where the texture of the blend was weaker than that of plain iPP. Moreover, in the texture of two-way drawn iPP one can observe some traces of orientation of crystallites with the *c* axis along the MD, and in other directions in the MD–TD plane which are remnants of the texture developed during the first drawing and the trace of reorientation path. In the blend sample such orientation was not detected. This is due to the larger amount of amorphous phase in the 8/2 blend than in plain iPP, which allows crystallites for less constrained rotations during the second drawing. As a result, practically all iPP crystallites in the blend rotate with their *c* axis to a new orientation direction, i.e. TD.

Figure 15 presents the two-dimensional SAXS patterns of two-way drawn iPP (*Figure 15a*) and 8/2 blend samples (*Figure 15b*) as well as the scans along the MD and TD (*Figures 15c* and *d*). There is almost no scattering from the lamellar structure in these patterns. One can distinguish only a weak trace of the 2-point pattern produced by scattering by lamellae oriented with their normals in the MD, which orientation was characteristic for the first stage of drawing, along the MD. It is apparent that the lamellar structure was destroyed during the second drawing, along the TD. As revealed by the WAXS pole figures the crystallites change their orientation by 90° rotation around the ND during this second drawing. These rotations are governed primarily by crystal slip mechanisms [the transverse slip systems on (010), (100), and (110) planes along with interlamellar sliding should be favoured at the beginning of redrawing, the chain slip mechanisms set in with some delay, necessary to produce some lamellae rotation first, possibly by interlamellar sliding]. The chain slip processes lead to thinning of lamellae and finally to breaking them into much smaller blocks[17]. Redrawing of already oriented material in the perpendicular direction should

induce such a destruction process at relatively low or moderate transverse strain. Further drawing after the destruction of lamellar structure leads to the perfection of crystalline texture, including further crystals rotation. The crystalline blocks emerging from that destruction process are very small and are positioned in space with too little correlation to give rise to small angle scattering of X-ray similar to that produced by the lamellar structure.

CONCLUSIONS

The two-stage drawing in orthogonal directions of plain iPP and iPP/HOCP blend leads to the formation of highly oriented films with well developed crystalline texture. The study of the mechanical properties revealed that the addition of HOCP to iPP up to 20 wt% greatly improves the properties of this polymer when highly oriented. On the other hand, the drawability of the iPP/HOCP blend films is almost as good as films of plain iPP and high strains can be easily achieved in both plain polypropylene and its blends with HOCP.

The multicomponent crystalline textures of both iPP and the blend obtained after one-way drawing are similar, both with chain axis oriented along MD. The texture of the blend is less developed than that of iPP, due to relatively higher activity of deformation mechanisms operating in the amorphous phase at the expense of those in the crystalline phase.

It was found that one-way drawing does not destroy the initial lamellar structure up to a strain of 4 and leads to the preferred orientation of lamellae with their normals coinciding with the *c* axis, both oriented in the MD.

The main active deformation mechanisms found on the basis of orientation studies are the (010)[001], (100)[001] and (110)[001] slip systems as well as {110} twinning mode. These mechanisms are supported by the deformation of amorphous phase by interlamellar sliding.

The second drawing in the transverse direction up to a strain of 7 leads to the formation in both iPP and iPP/HOCP blends of identical nearly one-component texture of the type (010)[001]. That texture is very sharp and well developed. The second texture element of the type of (110)[001] is much weaker than the principal one, so that the final texture of two-way drawn samples can be considered as a single-component. During the transverse drawing the lamellar structure of the films almost completely disappears due to breaking of lamellae into smaller crystallites.

Textural analysis leads to the conclusion that the easiest slip system in iPP monoclinic crystals is the chain slip of (010)[001]. Other active slip systems, (100)[001] and (110)[001], have higher critical resolved shear stress, which agrees with theoretical predictions. As a consequence, these slip systems lose in competition with the (010)[001] slip, which dominates at high strains. The final texture of two-way drawn samples suggests, however, that (110)[001] slip can be easier than (100)[001], which does not agree with the predictions.

ACKNOWLEDGEMENTS

This research was supported by the State Committee for Scientific Research (Poland) through the project 7S20401306. We are particularly grateful to Dr C. Silvestre and Dr S. Cimmino (IRTMP, Arco Felice) for supplying the oriented materials. We also thank Dr M. Pluta (CMMS, Łódź) and Dr T. Pakula (Max-Plank-Institüt für Polymerforschung, Mainz, FRG) for help in collection of SAXS data.

REFERENCES

1. Di Liello, V., Martuscelli, E., Ragosta, G. and Buzio, P., *J. Mater. Sci.*, 1989, **24**, 3235.
2. Marcandalli, B., Testa, G., Seves, A. and Martuscelli, E., *Polymer*, 1991, **32**, 3376.
3. Martuscelli, E., Silvestre, C., Canetti, M., De Lalla, C., Bonfatti, A. and Seves, A., *Makromol. Chem.*, 1989, **190**, 2615.
4. Martuscelli, E., Canetti, M. and Seves, A., *Polymer*, 1989, **30**, 304.
5. Cecere, A., Greco, R. and Taglialatela, A., *Polymer*, 1992, **33**, 1411.
6. Cimmino, S., Guarrata, P., Martuscelli, E., Silvestre, C. and Buzio, P., *Polymer*, 1991, **32**, 3299.
7. Cimmino, S., Di Pace, E., Karasz, F. E., Matuscelli, E. and Silvestre, C., *Polymer*, 1993, **34**, 972.
8. Krigbaum, W. R. and Uematsu, I., *J. Polym. Sci., Part A*, 1965, **3**, 767.
9. Alexander, L. E., *X-Ray Diffraction Methods in Polymer Science*. Wiley, New York, 1969, p. 198.
10. Ward, I. M. and Hadley, D. W., *An Introduction to the Mechanical Properties of Solid Polymers*. Wiley, New York, 1993, p. 221.
11. Cheng, S. Z. D., Janimiak, J. J. and Rodriguez, J., in *Polypropylene. Structure, Blends and Composites*, ed. J. Karger-Kocsis. Chapman & Hall, London, 1995, Vol. 1, Ch. 2.
12. Taraiya, A. K., Unwin, A. P. and Ward, I. M., *J. Polym. Sci. Polym. Phys. Ed.*, 1988, **26**, 817.
13. LaFrane, C. P. and Prud'homme, R. E., *Polymer* 1994, **35**, 3927.
14. Aboulfaraj, M., G'Sell, C., Ulrich, B. and Dahoun, A., *Polymer*, 1995, **36**, 731.
15. Frank, F. C., Keller, A. and O'Connor, A., *Phil. Mag.*, 1958, **3**, 64.
16. Triolo, A., Silvestre, C., Cimmino, S., Martuscelli, E., Caponetti, E., Floriano, M. A. and Triolo, R., *Abstracts of 5th European Symposium on Polymer Blends*, Maastricht, 1996, p. 411.
17. Galeski, A., Bartczak, Z., Argon, A. S. and Cohen, R. E., *Macromolecules*, 1992, **25**, 5705.